A00-16444

AIAA 2000-0574

MEASUREMENTS AND PREDICTIONS OF FLAME/STRETCH INTERACTIONS OF HYDROGEN-FUELED LAMINAR PREMIXED FLAMES

O. C. Kwon and G. M. Faeth
Department of Aerospace Engineering
The University of Michigan
Ann Arbor, MI

38th Aerospace Sciences
Meeting & Exhibit
10-13 January 2000 / Reno, NV

AIAA 2000-0574

MEASUREMENTS AND PREDICTIONS OF FLAME/STRETCH INTERACTIONS OF HYDROGEN-FUELED LAMINAR PREMIXED FLAMES

O.C. Kwon* G.M. Faeth†
Department of Aerospace Engineering
The University of Michigan
Ann Arbor, Michigan 48109-2140

Abstract

Fundamental unstretched laminar burning velocities, and flame response to stretch as characterized by Markstein numbers, were considered both experimentally and computationally for premixed laminar flames involving mixtures of hydrogen and oxygen with either nitrogen or argon as diluents. Outwardly-propagating spherical laminar premixed flames were considered for fuel-equivalence ratios of 0.6-4.5, pressures of 0.3-3.0 atm, and concentrations of O_2 in the nonfuel gases of 21% by volume at normal temperatures. The present flames were very sensitive to flame stretch, yielding ratios of stretched to unstretched laminar burning velocities in the range 0.8-3.0 for levels of flame stretch well below quenching conditions, e.g., for Karlovitz numbers less than 0.5. The agreement between measured and predicted unstretched laminar burning velocities and Markstein numbers was good using several contemporary reaction mechanisms. The resulting structure predictions suggest that H-atom production and transport is an important aspect of preferential-diffusion/stretch interactions, reflecting the strong correlation between laminar burning velocities and H-atom concentrations for present test conditions.

Nomenclature

A	=	pre-exponential factor
D	=	mass diffusivity
E_a	=	activation energy
(i)	=	mole fraction of species i
k	=	reaction coefficient
K	=	flame stretch or normalized increase of flame surface area, Eq. (3)
Ka	=	Karlovitz number, KD_u/S_L^2
L	=	Markstein length
Ma	=	Markstein number, L/δ_D
Ma_H	=	Markstein number based on $(H)_{max}$, Eq. (4)
n	=	power in reaction coefficient expression
P	=	pressure
r_f	=	flame radius
R	=	universal gas constant
S_L	=	laminar burning velocity based on unburned gas properties
S_L'	=	value of S_L at the largest radius observed
t	=	time
T	=	temperature
δ_D	=	characteristic flame thickness, D_u/S_L
ρ	=	density
ϕ	=	fuel-equivalence ratio
Subscripts		
b	=	burned gas
max	=	maximum observed value
u	=	unburned gas
∞	=	unstretched flame condition

Introduction

Recent studies of the effects of flame stretch on laminar premixed flames in this laboratory[1-7] were extended to consider hydrogen-fueled flames, seeking to manipulate preferential diffusion effects compared to

---

* Graduate Student Research Assistant, Department of Aerospace Engineering.

† Professor, Department of Aerospace Engineering, Fellow AIAA.

past work by varying flame pressures and diluents. Experimental observations of outwardly-propagating spherical laminar premixed flames were used to find laminar burning velocities as a function of flame stretch (represented by the Karlovitz number), the sensitivity of the laminar burning velocities to flame stretch (represented by the Markstein number), and the fundamental laminar burning velocities of unstretched (plane) flames. The measurements were also used to evaluate recently proposed detailed H_2/O_2 chemical reaction rate mechanisms due to Mueller et al.,[8] Marinov et al.,[9] and Frenklach et al.,[10] based on detailed numerical simulations of the same outwardly-propagating spherical laminar premixed flames as the experiments.

The fact that interactions between the preferential diffusion of various species and heat and flame stretch affect the structure, stability and speed of laminar premixed flames has been recognized for some time.[11-15] Recent studies have shown, however, that preferential-diffusion/stretch interactions are unusually strong, causing large variations of laminar burning velocities even for modest levels of stretch well away from quenching conditons.[1-7, 16-23] This provides strong motivation to study preferential-diffusion/stretch interactions, particularly for hydrogen-fueled flames where the chemistry is relatively simple and reasonably well known. Then detailed numerical simulations of stretched flames are computationally tractable and can help to provide insight about experimental results as well as the mechanisms of premixed flame sensitivity to stretch.

The present experiments were analyzed to find preferential-diffusion/stretch interactions similar to the earlier studies of outwardly-propagating spherical laminar premixed flames described in Ref. 1-7. As before, problems of flame thickness variations, curvature and unsteadiness caused by variations in laminar burning velocities with increasing flame radius were minimized during data reduction by only considering conditions where $\delta_D/r_f \ll 1$ and effects of ignition disturbances and radiative heat losses are small.[2-4] At such conditions, the relationship between the laminar burning velocity and flame stretch can be represented conveniently by combining an early proposal of Markstein[12] and the "local conditions" hypothesis of Kwon et al.,[1] to yield:

$$S_{L\infty}/S_L = 1 + MaKa \qquad (1)$$

where the dimensionless Karlovitz, Ka, and Markstein, Ma, numbers characterize flame stretch, and the response of the flame to stretch, respectively. The values of S_L and Ka were found following Strehlow and Savage,[13] based on predicted burned gas properties found using the computer codes of McBride et al. [24] and Reynolds,[25] as described later.

Several other proposals have been made to represent effects of flame stretch on laminar burning velocities, see Refs. 16-20 and references cited therein; nevertheless, Eq. (1) is particularly convenient because Ma has proven to be relatively constant for wide ranges of Ka. Thus, S_L and Ma provide concise measures of premixed flame propagation rates and response to stretch that will be used to summarize the findings of the present investigation. The small stretch limit of Eq. (1) is also of interest, in order to connect present results to classical asymptotic theories of laminar premixed flame propagation; this expression can be found from Eq. (1) as follows:[4]

$$S_L/S_{L\infty} = 1 - Ma_\infty Ka_\infty,\ Ka_\infty \ll 1 \qquad (2)$$

where $Ma_\infty \approx Ma$ has been observed for relatively wide ranges of Ka as noted earlier. Other advantages of the present characterization of premixed-flame/stretch interactions can be summarized as follows:[4] data reduction is direct and does not involve the use of flame structure models that are difficult to fully define and are likely to be revised in the future, the characterization is concise which facilitates its use by others, the positive and negative ranges of Ma provide a direct indication of stable and unstable flame surface conditions with respect to effects of preferential diffusion, and the results can be readily transformed to provide direct comparisons with other ways to characterize premixed-flame/stretch interactions. It should be noted, however, that the present approach has only been applied to outwardly-propagating spherical laminar premixed flames when δ_D/r_f, effects of ignition disturbances and effects of radiation are small. Thus, direct use of the present Ma to characterize effects of flame stretch for other circumstances should be approached with caution.

Past studies of interactions between stretched laminar premixed flames involving H_2 and O_2 as reactants are reviewed by Aung et al.[3,4] In addition, Aung et al.[3,4] extend measurements for H_2 and O_2 flames to consider effects of pressure and nitrogen

dilution on flame/stretch interactions and also complete numerical simulations of these flames finding reasonably good agreement between measurements and predictions based on the mechanisms of Frenklach et al.,[10] Kim et al.,[26] and Wang and Rogg.[27] Thus, the specific objectives of the present investigation were to consider further effects of pressure variations and dilution with argon and nitrogen in order to modify the transport environment of the flames compared to past work and to provide a new perspective for gaining a better understanding of premixed-flame/stretch interactions. In addition, while continuing evaluation of the mechanism of Frenklach et al.,[10] more recent mechanisms of Mueller et al.,[8] and Marinov et al.[9] were also considered during numerical simulations of flame properties.

The present discussion begins with descriptions of experimental and computational methods. Results are then considered, treating flame evolution and stability, flame response to stretch, unstretched laminar burning velocities, Markstein numbers, flame structure and effects of H-atom concentrations on flame behavior, in turn.

Experimental Methods

Apparatus

Experimental methods were similar to past work and will only be discussed briefly, see Refs. 1-7 for more details. The experiments were conducted in a spherical windowed chamber having an inside diameter of 360mm. The reactant mixture was prepared in the chamber by adding gases at appropriate partial pressures to reach the specified final pressure. The gases were mixed using a small metal fan located within the chamber with motion allowed to decay prior to ignition (10 minutes for both mixing and decay). The combustible mixture was spark-ignited at the center of the chamber using minimum spark ignition energies to control ignition disturbances. The flames were observed using high speed (up to 7000 pictures per second) motion picture shadowgraphy. Once combustion was complete, the chamber was vented and then flushed with air to remove condensed water vapor and cool the system to the allowable initial temperature range of the experiments (298±3K).

Data Reduction

Present measurements were limited to flames having diameters larger than 10 mm to avoid ignition disturbances and smaller than 60 mm to limit pressure increases during the measuring period to values less than 0.4% of the initial pressure. No results were considered where the flame surface was distorted or wrinkled due to effects of buoyancy or flame instability. Similar to earlier work, Refs. 1-7, measurements were limited to $\delta_D/r_f < 2\%$ so that effects of curvature and transient phenomena associated with large flame thicknesses were small. Finally, radiative heat losses were small due to the large flame speeds of hydrogen-fueled flames and were ignored similar to past work. For these conditions, the laminar burning velocity and flame stretch are given as follows:

$$S_L = (\rho_b/\rho_u)dr_f/dt, \quad K = (2/r_f)dr_f/dt \qquad (3)$$

The density ratio appearing in Eq. (3) was found from McBride et al.[24] and Reynolds[25] (both yielding the same results) which assumes adiabatic constant-pressure combustion with the same concentrations of elements in the unburned and burned gases. This is a convention that follows past practice which ignores preferential diffusion effects that modify local mixture fractions and energy transport and cause (ρ_b/ρ_f) to differ from plane flame conditions. The convention is convenient, however, because a single density ratio relates all flame speeds and the approach retrieves the correct flame displacement velocity, dr_f/dt, for given unburned mixture conditions and Ka. Given reliable flame structure predictions, however, density ratios can be found as a function of Ka so that actual laminar burning velocities and mass burning rates can be found; this work will be considered in the future pending successful evaluation of flame property predictions.

Final results were obtained by averaging measurements of 4-6 tests at each condition. The resulting experimental uncertainties (95% confidence) are as follows: S_L less than 10%, Ka less than 20%, and |Ma| less than 25% for |Ma| >1 and less than 25/|Ma|% for |Ma| <1.

Test Conditions

Experimental conditions involved reactant mixtures at normal temperature with fuel-equivalence ratios of 0.6-4.5, pressures of 0.3-3.0 atm, concentrations of oxygen in the nonfuel gases of 21% by volume, Karlovitz numbers of 0-0.5, ratios of stretched to unstretched laminar burning velocities of 0.8-3.0 and values of unstretched laminar burning velocities of 820-3500 mm/s.

Computational Methods

Numerical Simulations

Computational methods for the present flames were similar to those used by Aung et al.[3,4] The outwardly-propagating spherical flames were simulated using the unsteady, one-dimensional laminar flame computer code RUN-IDL developed by Rogg.[28] This algorithm allows for mixture-averaged multi-component diffusion, thermal diffusion, variable thermochemical properties, and variable transport properties. The CHEMKIN package[29-31] was used as a preprocessor to find the thermochemical and transport properties for RUN-IDL. Transport properties were found following Hirschfelder and Curtiss[32] using the transport property data base of Kee et al.;[31] thermochemical properties were found from the thermodynamic data base of Kee et al.,[29] except for HO_2 where the recommendations of Kim et al.[26] were used. Prior to computing flame properties, all transport and thermochemical properties computed using the results of Refs. 29, 30 and 31 were checked against original sources. Effects of radiation were small due to the large flame velocities of hydrogen-fueled flames and were ignored. Flame propagation was allowed to proceed sufficiently far so that effects of initial conditions were small, similar to the measurements. Other limitations used to control experimental uncertainties, e.g., $\delta_D/r_f<2\%$, etc., were also applied to the predictions. Finally, the computational grid in space and time was varied to ensure numerical accuracy within 1%, estimated by Richardson extrapolation of S_L. The numerical simulations were analyzed similar to the measurements, taking the flame position at the point where gas temperatures were the average of the hot and cold boundaries. Due to stringent flame thickness limitations, however, the results were not affected significantly by the criterion used to define the flame positions.

Separate calculations were completed for unstretched (plane) flames using the steady one-dimensional laminar premixed flame code, PREMIX, of Kee and coworkers.[33] This code allowed evaluation of effects of the use of the mixture-averaged multi-component diffusion approximation; similar to the findings of Aung et al.[3,4] use of the mixture-averaged multicomponent mass diffusion approximation while including effects of thermal diffusion yielded errors of predicted flame properties much smaller than experimental uncertainties and this procedure was used for the RUN-IDL calculations.

Chemical Reaction Mechanism

Three relatively recent H/O reaction mechanisms were considered, as follows: Mueller et al.,[8] Marinov et al.,[9] and Frenklach et al.[10] C/H/O and N/O chemistry were not important for present conditions, similar to the findings of Aung et al., [3,4] and were deleted from the mechanisms. Finally, an updated version of the mechanism of Marinov et al.[9] was used, see Table 1 for a summary of the specific changes from the original source.

The final reduced chemical reaction mechanisms, after incorporating the simplifications just discussed, involved 10 species and 19 reversible reactions for the approach of Mueller et al.,[8] 20 reversible reactions for the approach of Marinov et al.,[9] and 25 reversible reactions for the approach of GRI-Mech 2.1 developed by Frenklach et al.,[10] not counting the range of third body collision efficiencies that were used. The backward rates for all the mechanisms were found from chemical equilibrium requirements using the CHEMKIN package.[30]

Results and Discussion

Flame Stability and Evolution

Three kinds of flame surface instabilities were observed: preferential-diffusion instability (when $Ma < 0$), hydrodynamic instability and buoyant instability. Shadowgraph photographs of flame surface after distortion by these instabilities for outwardly-propagating spherical flames appear in Kwon et al.[1] and references cited therein. The presence of

preferential-diffusion instability could be identified by irregular (chaotic) distortions of the flame surface relatively early in the flame propagation process. Hydrodynamic instability could be identified by the development of a somewhat regular cellular disturbance pattern on the flame surface, rather late in the flame propagation process, similar to the observations of Groff.[34] Finally, buoyant instabilities were readily detected by distortion of the flame surface from a spherical shape, as well as by upward motion of the centroid of the flame image. As noted earlier, no measurements were made when any of these instabilities were observed.

Flame Response to Stretch

Results for finite flame radii involve finite values of flame stretch; therefore, values of $S_{L\infty}$ were found by extrapolating the measurements to Ka = 0 similar to past work.[1-7] Then given $S_{L\infty}$, plots of $S_{L\infty}/S_L$ as a function of Ka can be constructed for various values of ϕ as suggested by Eq. (1). A sample of such results for H_2/21% O_2/Ar flames (i.e., oxygen concentrations of 21% by volume in the nonfuel gases) at normal temperature and pressure (NTP) with ϕ = 0.60, 0.90, 1.50 and 3.75 is illustrated in Fig. 1. Results at all other test conditions are qualitatively similar.

Results of both measurements and predictions illustrated in Fig. 1 exhibit the linear relationships between $S_{L\infty}/S_L$ and Ka that was exploited to find $S_{L\infty}$; similar linear behavior was observed during earlier work, see Refs. 1-7. The slope of these plots is equal to Ma according to Eq. (1) which already is independent of Ka over the range of the measurements. Similar behavior was observed over the present test range, which involves Ka < 0.5, however, quenching effects as extinction conditions are approached (where Ka would be on the order of unity, see Law[15]) would probably yield a more complex response to stretch. Even for the present modest range of Ka, however, effects of flame stretch on S_L were significant, e.g., over the entire test range, $S_{L\infty}/S_L$ varied in the range 0.8-3.0 for Ka < 0.5.

The predictions illustrated in Fig. 1 were based on the mechanism of Mueller et al.[8] but results using the Marinov et al.[9] and Frenklach et al.[10] mechanisms were similar. The results of the numerical simulations are shown to be qualitatively similar to the measurements supporting a linear variation of $S_{L\infty}/S_L$ with increasing Ka and similar values of ϕ for unstable (Ma < 0) and stable (Ma > 0) preferential-diffusion behavior.

Unstretched Laminar Burning Velocities

In the following, measured values of laminar burning velocities will be limited to results that have been corrected to provide $S_{L\infty}$. Measurements and predictions of $S_{L\infty}$ as a function of fuel-equivalence ratio for hydrogen/air flames at NTP are plotted in Fig. 2. Measurements shown on the figure include results of Taylor,[16] Karpov et al.,[19] Egolfopoulos and Law,[21] Vagelopoulos et al.,[22] Aung et al.[3] and the present investigation. Predictions shown on the plot included results of Sun et al.[23] for unstretched flames using an integral method and the mechanism of Kim et al.[26] as well as present predictions for the reaction mechanisms of Refs. 8-10 found by extrapolating results for simulations of outwardly-propagating spherical flames similar to the measurements. It should be noted that the mechanism of Kim et al.[26] was used by Aung et al.[3,4] and is an earlier version of Mueller et al.[8] used during the present investigation. The measurements generally agree within experimental uncertainties whereas measurements and all the predictions are in good agreement for fuel-lean conditions. At fuel-rich conditions, the predictions of Frenklach et al. (GRI-MECH-2.1)[10] and Sun et al.[23] are somewhat larger than the measurements; nevertheless, the GRI-MECH predictions are still surprisingly good even though this mechanism was not particularly tailored for hydrogen-fueled flames. The predictions of Sun et al.[23] are very similar to the earlier predictions of Aung et al.[3,4] using the same mechanism in conjunction with a numerical simulation of the propagating flame.

Measurements of laminar burning velocities were carried out replacing the nitrogen in air with argon. The specific heats of argon are smaller than nitrogen which provide a way to consider effects of larger flame temperatures on flame/stretch interactions. The corresponding measurements and predictions of $S_{L\infty}$ as a function of fuel-equivalence ratio are plotted in Fig. 3. In this case, only results from the present study are available with the three predictions obtained from the mechanisms of Refs. 8-10, as before. Comparing Figs. 2 and 3 shows that replacing nitrogen with argon yields roughly a 25% increase of the maximum

unstretched laminar burning velocity but with little change in the value of the fuel-equivalence ratio where the maximum is observed, e.g., $\phi \approx 1.8$. All the predictions reproduce this trend but the mechanism of Mueller et al.[8] is seen to provide the best quantitative predictions over the entire test range of Figs. 2 and 3.

Markstein Numbers

As discussed earlier, Markstein numbers are independent of Karlovitz numbers for present conditions and can be plotted as a function of reactant conditions only. Measured and predicted values of Markstein numbers for hydrogen/air flames at NTP are plotted as a function of fuel-equivalence ratio in Fig. 4. Measurements shown on the figure include the results of Taylor,[16] Karpov et al.,[19] Aung et al.[3] and the present investigation. Predictions shown on the plot include results of Sun et al.[23] and the present investigation. Over the range of conditions where $\delta_D/r_f < 2\%$, the various measurements agree within experimental uncertainties. Outside this range for very lean $\phi < 0.60$ and very rich $\phi > 5.0$ flames, discrepancies among the various measurements become relatively large, reflecting the larger experimental uncertainties and the intrusion of other effects (e.g., transient phenomena) on measured values of Markstein numbers. Similar to the results for unstretched laminar burning velocities in Fig. 2, all the measurements and predictions are in reasonably good agreement for fuel-lean conditions. Discrepancies among the predictions are somewhat larger at fuel-rich conditions with present predictions using all three mechanisms being somewhat smaller than that of Sun et al.[23] Earlier predictions of Aung et al.[3] using the Kim et al.[26] mechanism used by Sun et al.[23] are also similar to the present results so the reason for these differences remain unknown. The general characteristics of unstable behavior ($Ma < 0$) at fuel-lean conditions and stable behavior ($Ma > 0$) at fuel-rich conditions are consistent with conventional explanations based on preferential diffusion of the deficient reactant, see Refs. 1 and 3 and references therein. Behavior at intermediate conditions (between $\phi \approx 1$ where $Ma = 0$ and $\phi \approx 1.8$ where $S_{L\infty}$ reaches a maximum) is more complex, however, and must involve preferential diffusion of both heat and mass. Another interesting feature of the results illustrated in Fig. 4 is the extended plateau region where Ma varies slowly between $\phi \approx 2$ and 5 even though present experiments did not approach flammability limits. It is encouraging that the numerical simulations based on detailed chemical mechanisms can reproduce these trends, even though Markstein numbers were not used during past efforts to optimize the chemical kinetic parameters of these mechanisms. An attempt to exploit the predictions in order to obtain a better fundamental understanding of the behavior of Markstein numbers for hydrogen-fueled flames will be discussed later.

Corresponding measurements and predictions of Markstein numbers for hydrogen-fueled flames when nitrogen is replaced by argon at NTP are illustrated in Fig. 5. As before, only measurements and predictions from the present study are available for these conditions. Comparing Figs. 4 and 5 shows that replacing nitrogen with argon has remarkably little effect on either the trends or magnitudes of the Markstein numbers. Computations using all three mechanisms reproduce this behavior very well, which is encouraging.

Effects of pressure on Markstein numbers were also investigated. Aung et al.[4] present extensive results for variations of Markstein numbers with pressure and fuel-equivalence ratios for hydrogen/air flames at pressures of 0.35-4.00 atm and normal temperature. These results suggest reasonably good agreement between measurements and predictions and relatively small effects of pressure on the magnitude and trends of Markstein numbers. Present predictions using the newer mechanisms of Refs. 8 and 9, indicated similar behavior. Present measurements and predictions of Markstein numbers as a function of pressure for hydrogen-fueled flames where nitrogen has been replaced by argon are illustrated in Fig. 6. These results are very similar to the hydrogen/air results of Aung et al.:[4] measurements and predictions agreed reasonably well and pressure variations do not have a large effect on Markstein number values for pressures of 0.3-3.0 atm.

Flame Structure

Measurements and predictions of $S_{L\infty}$ and Ma are in reasonably good agreement over the present test range; therefore, the predictions were exploited to seek improved understanding about flame/stretch interactions. Results of this type for flames where nitrogen has been replaced by argon are discussed in

the following based on the Mueller et al.[8] mechanism. Corresponding results based on the mechanisms of Marinov et al.[9] and Frenklach et al.[10] were similar. Similar results for hydrogen/air flames can be found in Aung et al.[3] The approach involved numerical simulations of outwardly-propagating spherical flames for unstable (ϕ = 0.6) and stable (ϕ = 4.5) preferential-diffusion conditions. Flame-structure/stretch interactions were observed by comparing results for a moderate level of stretch (Ka = 0.07) with corresponding predictions for unstretched (plane) flames.

Typical predicted structures of stretched and unstretched laminar premixed H_2/21% O_2/Ar flames at NTP are illustrated in Figs. 7 and 8 for unstable and stable conditions, respectively. Results illustrated in the figures include distributions of temperature and species concentrations as a function of distance though the flame. (Note that the origins of the length scales for unstretched and stretched flames are arbitrary and do not correspond to the central ignition point.)

Considering the results for the unstable flame in Fig. 7, finite levels of stretch cause flame temperatures to increase. This occurs because the faster diffusing hydrogen compared to oxygen causes the flame to become more nearly stoichiometric. (note the reduced concentrations of oxygen and increased concentrations of water vapor at the hot boundary of the stretched flame compared to the unstretched flame); this causes a corresponding increase of flame temperatures of the stretched flame compared to the unstretched flame. The increased temperature (and possibly increased hydrogen atom concentrations) causes radical concentrations in the reaction zone of the stretched flame to increase compared to the unstretched flame (e.g., the maximum mole fraction of H in the stretched and unstretched flames are roughly 0.020 and 0.017, respectively), increasing reaction rates and thus laminar burning velocities for the stretched flame.

The effect of stretch on flame structure for stable conditions is just opposite to the behavior just discussed for unstable conditions (compare Figs. 7 and 8). For stable conditions, finite levels of stretch cause flame temperatures to decrease. This occurs because the faster-diffusing hydrogen compared to oxygen causes the flame to become even richer (note the increased concentrations of H_2 and decreased concentrations of water vapor at the hot boundary of the stretched flame compared to the unstretched flame); this causes a corresponding reduction of flame temperatures of the stretched flame compared to the unstretched flame. The reduced temperature (somewhat opposed by increased hydrogen atom concentrations) causes radical concentrations in the reaction zone of the stretched flame to decrease compared to the unstretched flame (e.g., the maximum mole fractions of H in the stretched and unstretched flames are roughly 0.026 and 0.033, respectively) decreasing reaction rates and thus laminar burning velocities for the stretched flames.

Similar to the behavior of hydrogen/air flames, discussed by Aung et al.,[3] effects of flame structure on H_2/21% O_2/Ar flames at NTP are more complex at intermediate fuel-equivalence ratios near the maximum laminar burning velocity condition (where effects of fuel-equivalence ratio on the laminar burning velocity are weaker than for more fuel-lean and fuel-rich conditions). In this intermediate regime, effects of preferential diffusion of heat and mass, as well as the tendency of increased hydrogen concentrations in the reaction zone to increase radical concentrations there, become factors in addition to effects of preferential diffusion that were just discussed. Consideration of effects of radicals on laminar burning velocities helps provide insight about this behavior that will be considered next.

H-Atom Behavior

The results of Figs. 7 and 8 indicate that H-atom has the largest concentrations of all radicals in the reaction zone of the present flames, even for lean flames with fuel-equivalence ratios as small as ϕ = 0.6, the smallest value considered during the present study. In addition, Padley and Sugden[35] established a strong correlation between laminar burning velocities and H-atom concentrations for $H_2/O_2/N_2$ flames based on their direct measurements of radial concentrations and the laminar burning velocity measurements of Jahn.[36] Combining these observations with the fact that H-atom has significantly larger diffusivities than those of other species and heat in the present H_2/O_2/diluent flames tends to implicate this radical as an important factor in the relatively strong flame/stretch interactions observed for present test conditions. The following discussion seeks to quantify this H-atom preferential diffusion mechanism.

Present computations were used to study the correlation between laminar burning velocities and maximum H-atom concentrations. These results are illustrated in Fig. 9. Present predictions shown on the plot involve all fuel-equivalence ratios and pressures for flames using both nitrogen and argon as diluents, and includes results for both stretched and unstretched flames. This large range of conditions yields a somewhat scattered but still quite strong correlation between laminar burning velocities and maximum H mole fractions. The present correlation is qualitatively similar to the correlation reported by Padley and Sugden,[35] which is also shown on the plot.

The behavior observed in Fig. 9 suggests that maximum H-atom concentrations could serve as a surrogate for the laminar burning velocity when considering flame/stretch interactions. This behavior is explored in Fig. 10 where the ratios of the unstretched-to-stretched maximum H mole fractions are plotted as a function of Karlovitz numbers, analogous to the plot of $S_{L\infty}/S_L$ as a function of Karlovitz number in Fig. 1. Effects of diluent are also shown on the plot, with results for H_2/air flames shown at the top and results for H_2/21% O_2/Ar flames shown at the bottom, both for reactants at NTP. Three sets of results are shown for each diluent, spanning the present range of fuel-equivalence ratios; results for other conditions are similar. Remarkably, these plots are linear, similar to the laminar burning velocity results of Fig. 1, and numerous other measurements of laminar burning velocities reported in Refs. 1-7. This behavior suggests defining an expression for the effects of stretch on maximum H-atom concentrations, analogous to Eq. (1), as follows:

$$(H)_{max\infty}/(H)_{max} = 1 + Ma_H Ka \qquad (4)$$

The behavior of Ma_H was studied by plotting the correlation between Ma_H and Ma as illustrated in Fig. 11. Results shown on the plot consider the full range of present test conditions at normal temperature (NT). Based on the results illustrated in Fig. 10, the correlation of Fig. 11 includes stretched flames, extending up to the maximum stretch values considered during the present investigation. The strong correlation between Ma and Ma_H is evident, supporting the importance of H-atom concentrations for the preferential diffusion effects causing the flame/stretch interactions observed during the present investigation. These results suggest, however, that other factors are involved, e.g., the correlation is not linear and conditions where Ma and $Ma_H = 0$ do not coincide. Thus, additional study is needed to better understand the mechanism of flame/stretch interactions, even in relatively simple H_2/O_2/diluent flames.

Conclusions

Effects of positive flame stretch on the laminar burning velocities of flames involving $H_2/O_2/N_2$ or Ar mixtures were studied experimentally and computationally. The experiments involved outwardly-propagating laminar spherical flames similar to past work in this laboratory, see Refs. 1-7; the computations involved numerical simulations of the same flame configuration considering detailed reaction mechanisms due to Mueller et al.,[8] Marinov et al.,[9] and Frenklach et al.[10] The reactant mixtures were at normal temperature with fuel-equivalence ratios of 0.6-4.5, pressures of 0.3-3.0 atm, concentrations of oxygen in nonfuel gases of 21% by volume, Karlovitz numbers of 0-0.5 and ratios of unstretched/stretched laminar burning velocities of 0.8-3.0. The major conclusions of the study are as follows:

1. Effects of flame/stretch interactions for both measurements and predictions could be correlated based on the local conditions hypothesis according to $S_{L\infty}/S_L = 1 + MaKa$ to obtain a linear relationship between $S_{L\infty}/S_L$ and Ka, yielding Markstein numbers that were constants for given reactant conditions.
2. Effects of flame stretch on laminar burning velocities were substantial, yielding Markstein numbers in the range –2 to 5.
3. Predicted and measured unstretched laminar burning velocities and Markstein numbers were in good agreement using reaction mechanisms due to Mueller et al.,[8] Marinov et al.[9] and Frenklach et al..[10]
4. Predictions show that stretched and unstretched flames exhibit a strong correlation between laminar burning velocities and H-atom concentrations similar to the measurements of Padley and Sugden[35] in similar flames.
5. The local conditions hypothesis provides a simple correlation between unstretched/stretched maximum H-atom concentrations and the

Karlovitz number similar to the behavior of laminar burning velocities, yielding constant H-Markstein numbers for particular reactant conditions.

6. The corresponding strong correlation between H-Markstein numbers suggests that H-atom production and transport is an important aspect of preferential diffusion/stretch interactions which is not surprising in view of the unusually large diffusivity and strong effect on laminar burning velocities of this light radical.

Acknowledgments

This research was supported in part by NSF Grant CTS-9321959 under the Technical Management of F. Fisher. Support from the Rackham Fellowship Program of the University of Michigan for O.C. Kwon is also gratefully acknowledged.

References

[1]Kwon, S., Tseng, L.-K., and Faeth, G.M., "Laminar Burning Velocities and Transition to Unstable Flames in $H_2/O_2/N_2$ and $C_3H_8/O_2/N_2$ Mixtures," Combust. Flame, Vol. 90, No. 3, 1992, pp. 230-246.

[2]Tseng, L.-K., Ismail, M.A., and Faeth, G.M., "Laminar Burning Velocities and Markstein Numbers of Hydrocarbon/Air Flames," Combust. Flame, Vol. 95, No. 4, 1993, pp. 410-426.

[3]Aung, K.T., Hassan, M.I., and Faeth, G.M., "Flame/Stretch Interactions of Laminar Premixed Hydrogen/Air Flames at Normal Temperature and Pressure," Combust. Flame, Vol. 109, No. 1/2, 1997, pp. 1-24.

[4]Aung, K.T., Hassan, M.I., and Faeth, G.M., "Effects of Pressure and Nitrogen Dilution on Flame/Stretch Interactions of Laminar Premixed $H_2/O_2/N_2$ Flames," Combust. Flame, Vol. 112, No. 1/2, 1998 pp. 1-15.

[5]Hassan, M.I., Aung, K.T., and Faeth, G.M., "Measured and Predicted Properties of Laminar Premixed Methane/Air Flames at Various Pressures," Combust. Flame, Vol. 115, No. 4, 1998, pp. 539-550.

[6]Hassan, M.I., Aung, K.T., Kwon, O.C., and Faeth, G.M., "Properties of Laminar Premixed Hydrocarbon/Air Flames at Various Pressures," J. Prop. Power, Vol. 14, No. 4, 1998, pp. 479-488.

[7]Kwon, O.C., Hassan, M.I., and G.M. Faeth, "Flame/Stretch Interactions of Premixed Fuel-Vapor/O_2/N_2 Flames," J. Prop. Power, in press.

[8]Mueller, M.A., Kim, T.J., Yetter, R.A., and Dryer, F.L., "Flow Reactor Studies and Kinetic Modeling of the H_2/O_2 Reaction," Int. J. Chem. Kinetics, Vol. 31, No. 2, 1999, pp. 113-125.

[9]Marinov, N.M., Westbrook, C.K., and Pitz, W.J., "Detailed and Global Chemical Kinetics Model for Hydrogen," *Transport Phenomena in Combustion* (S.H. Chan, ed.), Vol. 1, Taylor & Francis, Washington, DC, 1996, pp. 118-129.

[10]Frenklach, M., Wang, H., Bowman, C.T., Hanson, R.K., Smith, G.P., Goldin, D.M., Gardiner, W.C., and Lissianski V., "An Optimized Kinetics Model for Natural Gas Combustion," World Wide Web, http://www.gri.org/Basic Research/GRI-Mech, Version 2.1, 1995.

[11]Manton, J., von Elbe, G., and Lewis, B., "Nonisotropic Propagation of Combustion Waves in Explosive Gas Mixtures and Development of Cellular Flames," J. Chem. Phys. Vol. 20, 1952, pp. 153-158.

[12]Markstein, G.H., *Non-Steady Flame Propagation*, Pergamon, New York, 1964, p. 22.

[13]Strehlow, R.A., and Savage, L.D., "The Concept of Flame Stretch," Combust. Flame, Vol. 31, No. 2, 1978, pp. 209-211.

[14]Clavin, P., "Dynamic Behavior of Premixed Flame Fronts in Laminar and Turbulent Flows," Prog. Energy Combust. Sci., Vol. 11, No. 1, 1985 , pp. 1-59.

[15]Law, C.K., "Dynamics of Stretched Flames," *Twenty-Second Symposium (International) on Combustion*. The Combustion Institute, Pittsburgh, 1988, pp. 1381-1402.

[16]Taylor, S.C., "Burning Velocity and Influence of Flame Stretch," Ph.D. Thesis, University of Leeds, England, UK, 1991.

[17]Dowdy, D.R., Smith, D.B., Taylor, S.C., and Williams, A., "The Use of Expanding Spherical Flames to Determine Burning Velocities and Stretch Effects on Hydrogen/Air Mixtures," *Twenty-Third Symposium (International) on Combustion*, The Combustion Institute, Pittsburgh, 1990, pp. 325-333.

[18]Brown, M.J., McLean, I.C., Smith, D.B., and Taylor, S.C., "Markstein Lengths of CO/H_2/Air Flames, Using Expanding Spherical Flames," *Twenty-Sixth Symposium (International) on Combustion*, The Combustion Institute, Pittsburgh, 1996, pp. 875-882.

[19]Karpov, V.P., Lipatnikov, A.N., and Wolanski, P., "Finding the Markstein Number Using the Measurements of Expanding Spherical Laminar Flames," Combust. Flame, Vol. 109, No. 3, 1996, pp. 436-448.

[20]Bradley, D., Hicks, R.A., Lawes, M., Sheppard, C.G.W., and Woolley, R., "The Measurement of Laminar Burning Velocities and Markstein Numbers for Iso-Octane-Air and Iso-Octane-n-Heptane in Air Mixtures at Elevated Temperatures and Pressures in an Explosion Bomb," Combust. Flame, Vol. 115, No. 1/2, 1998, pp. 126-144.

[21]Egolfopoulos, F.N., and Law, C.K., "An Experimental and Computational Study of the Burning Rates of Ultra-Lean to Moderately-Rich $H_2/O_2/N_2$ Laminar Flames with Pressure Variations," *Twenty-Third Symposium (International) on Combustion,* The Combustion Institute, Pittsburgh, 1990, pp. 333-340.

[22]Vagelopoulos, C.M., Egolfopoulos, F.N., and Law, C.K.,"Further Considerations on the Determination of Laminar Flame Speeds with the Counterflow Twin-Flame Technique," *Twenty-Fifth Symposium (International) on Combustion*, The Combustion Institute, Pittsburgh, 1994, pp. 1341-1347.

[23]Sun, C.J., Sung, C.J., He, L., and Law, C.K., "Dynamics of Weakly Stretched Flames: Quantitative Description and Extraction of Global Flame Parameters," Combust. Flame, Vol. 118, No. 1/2, 1999, pp. 108-128.

[24]McBride, B.J., Reno, M.A., and Gordon, S., "CET93 and CETPC: An Interim Updated Version of the NASA Lewis Computer Program for Calculating Complex Chemical Equilibrium with Applications," NASA Technical Memorandum 4557, 1994.

[25]Reynolds, W.C., "The Element Potential Method for Chemical Equilibrium Analysis: Implementation in the Interactive Program STANJAN," Department of Mechanical Engineering Report, Stanford University, Stanford, CA, 1986.

[26]Kim, T.J., Yetter, R.A., and Dryer, F.L., "New Results on Moist CO Oxidation: High Pressure, High Temperature Experiments and Comprehensive Kinetic Modeling," *Twenty-Fifth Symposium (International) on Combustion*, The Combustion Institute, Pittsburgh, 1994, pp. 759-766.

[27]Wang, W., and Rogg, B., "Reduced Kinetic Mechanisms and Their Numerical Treatment I: Wet CO Flames," Combust. Flame, Vol. 94, 1993, pp. 271-292.

[28]Rogg, B., "RUN-1DL: The Cambridge Universal Laminar Flame Code," Technical Report CUED/A-THERMO/TR39. Department of Engineering, University of Cambridge, England, UK, 1991.

[29]Kee, R.J., Rupley, F.M., and Miller, J.A., "The CHEMKIN Thermodynamic Data Base," Report No. SAND87-8215B. Sandia National Laboratories, Albuquerque, NM, 1992.

[30]Kee, R.J., Rupley, F.M., and Miller, J.A., "CHEMKIN II: A Fortran Chemical Kinetics Package for the Analysis of Gas Phase Chemical Kinetics," Report No. SAND89-8009B, Sandia National Laboratories, Albuquerque, NM, 1993.

[31]Kee, R.J., Dixon-Lewis, G., Warnatz, J., Coltrin, M.E., and Miller, J.A., "A FORTRAN Computer Code Package for the Evaluation of Gas-Phase, Multi-component Transport Properties," Report No. SAND86-8246, Sandia National Laboratories, Albuquerque, NM, 1992.

[32]Hirschfelder, J.O., and Curtiss, C.F., "Theory of Propagation of Flames. Part I: General Equations," *Third Symposium on Combustion and Flame and Explosion Phenomena*, The Combustion Institute, Pittsburgh, 1948, pp. 121-127.

[33]Kee, R.J., Grcar, J.F., Smooke, M.D., and Miller, J.A., "A FORTRAN Program for Modeling Steady Laminar One-Dimensional Premixed Flames," Report No. SAND85-8240, Sandia National Laboratories, Albuquerque, NM, 1993.

[34]Groff, E.G., "The Cellular Nature of Confined Spherical Propane-Air Flames," Combust. Flame, Vol. 48, 1982, pp. 51-62.

[35]Padley, P.J., and Sugden, T.M., "Chemiluminescence and Radical Recombination in Hydrogen Flames," *Seventh Symposium (International) on Combustion*, The Combustion Institute, Pittsburgh, PA, 1958, pp. 235-244.

[36]Jahn, G., cited in Lewis, B., and von Elbe, G., *Combustion, Flames and Explosions of Gases*, 3rd ed., Academic Press, New York, 1987, pp. 395-402.

Table 1. Corrections of Marinov et al.[9] Mechanism[a]

No.	Reaction	A	n	E_a
5b	$H+H+H_2 = H_2+H_2$	9.20E+16	-0.6	0.0
7	$H+O+M = OH+M^b$	4.71E+18	-1.0	0.0
8	$H+OH+M = H_2O+M^b$	2.21E+22	-2.0	0.0
10	$H+HO_2 = H_2+O_2$	6.63E+13	0.0	2.126
14	$OH+HO_2 = H_2O+O_2^c$	2.13E+28	-4.827	3.500
	$OH+HO_2 = H_2O+O_2^c$	9.10E+14	0.0	10.964

[a]H_2/O_2 reaction mechanism with equations numbered same as original source; all other equations unchanged from original source. Units are cm^3/gmol/s/kcal/K and the reaction coefficient is taken as $k = AT^n \exp(-E_a/RT)$.

[b]Efficiency factors for the collision partners of this reaction are 6.4 for H_2O, all other species have efficiency factors of unity.

[c]This reaction is expressed as the sum of the two rate expressions.

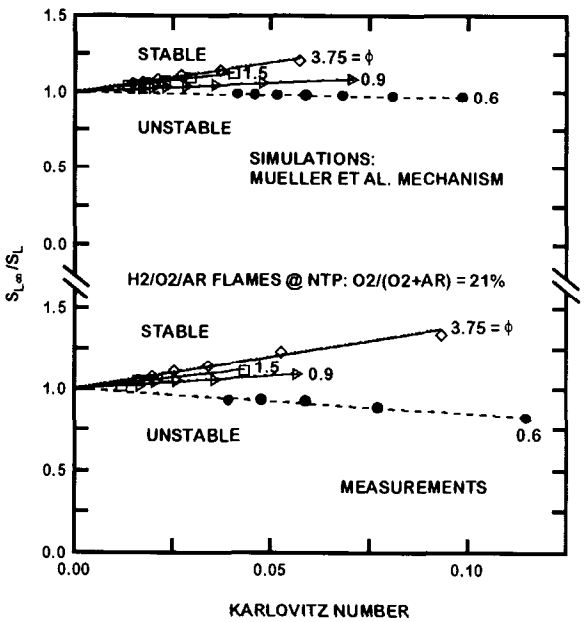

Fig. 1. Measured and predicted laminar burning velocities as a function of Karlovitz number and fuel-equivalence ratio for H_2/21% O_2/Ar flames at NTP.

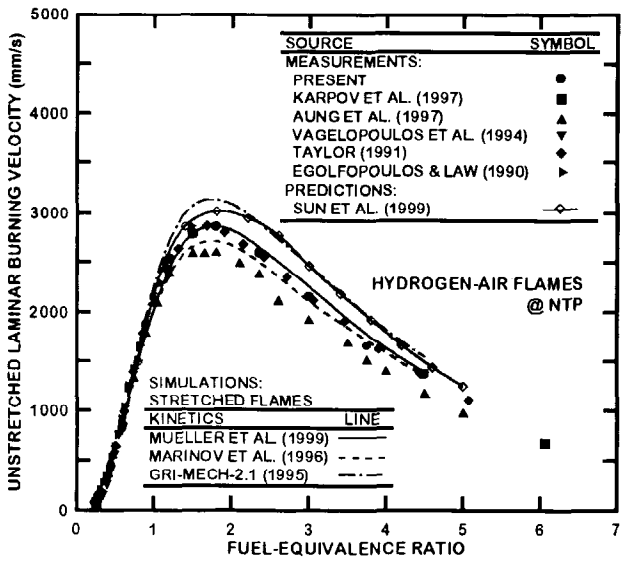

Fig. 2. Measured and predicted unstretched laminar burning velocities as a function of fuel-equivalence ratio for hydrogen/air flames at NTP. Measurements of Karpov et al.,[19] Aung et al.,[3] Vagelopoulos et al.,[22] Taylor,[16] Egolfopoulos and Law[21] and the present investigation; predictions of Sun et al.[23] and the present investigation.

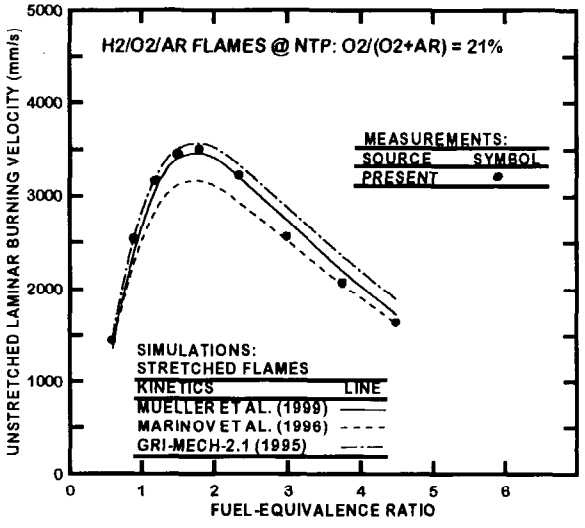

Fig. 3. Measured and predicted unstretched laminar burning velocities as a function of fuel-equivalence ratio for H_2/21% O_2/Ar flames at NTP.

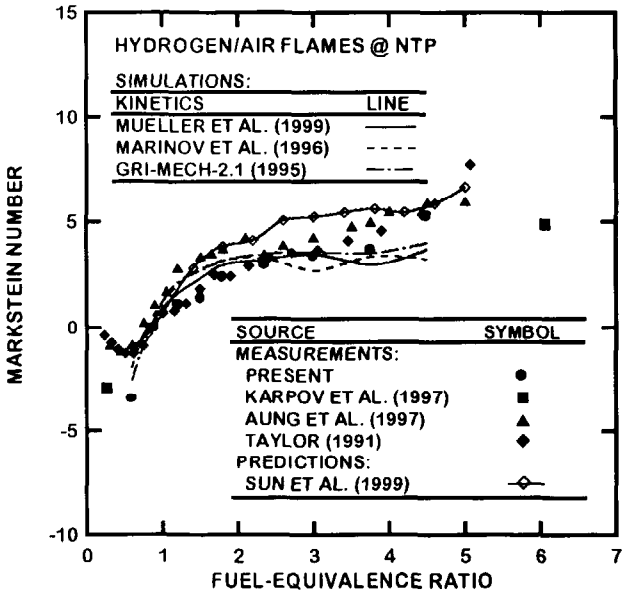

Fig. 4. Measured and predicted Markstein numbers as a function of fuel-equivalence ratio for hydrogen/air flames at NTP. Measurements of Karpov et al.,[19] Aung et al.,[3] Taylor,[16] and the present investigation.

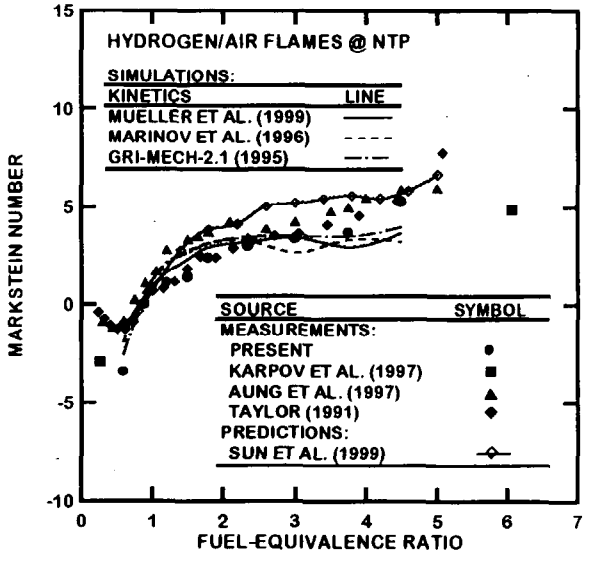

Fig. 5. Measured and predicted Markstein numbers as a function of fuel-equivalence ratio for H_2/21% O_2/Ar flames at NTP.

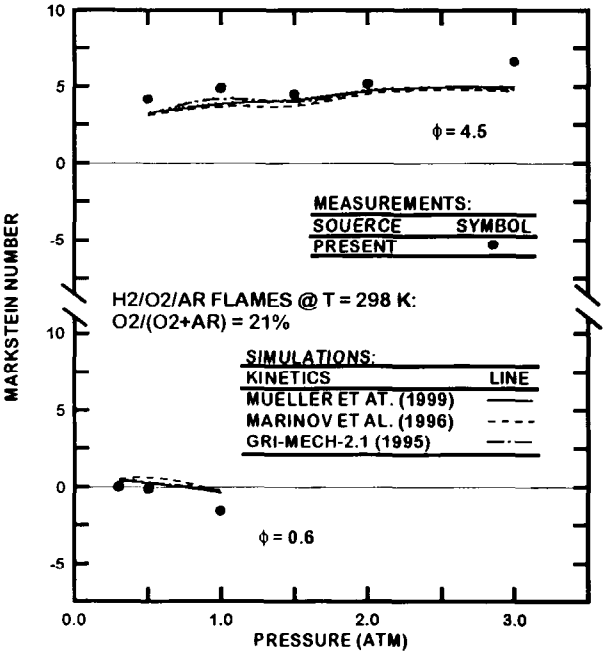

Fig. 6. Measured and predicted Markstein numbers as a function of pressure for H_2/21% O_2/Ar flames at fuel-equivalence ratios of 0.6 and 4.5 and a temperature of 298 K.

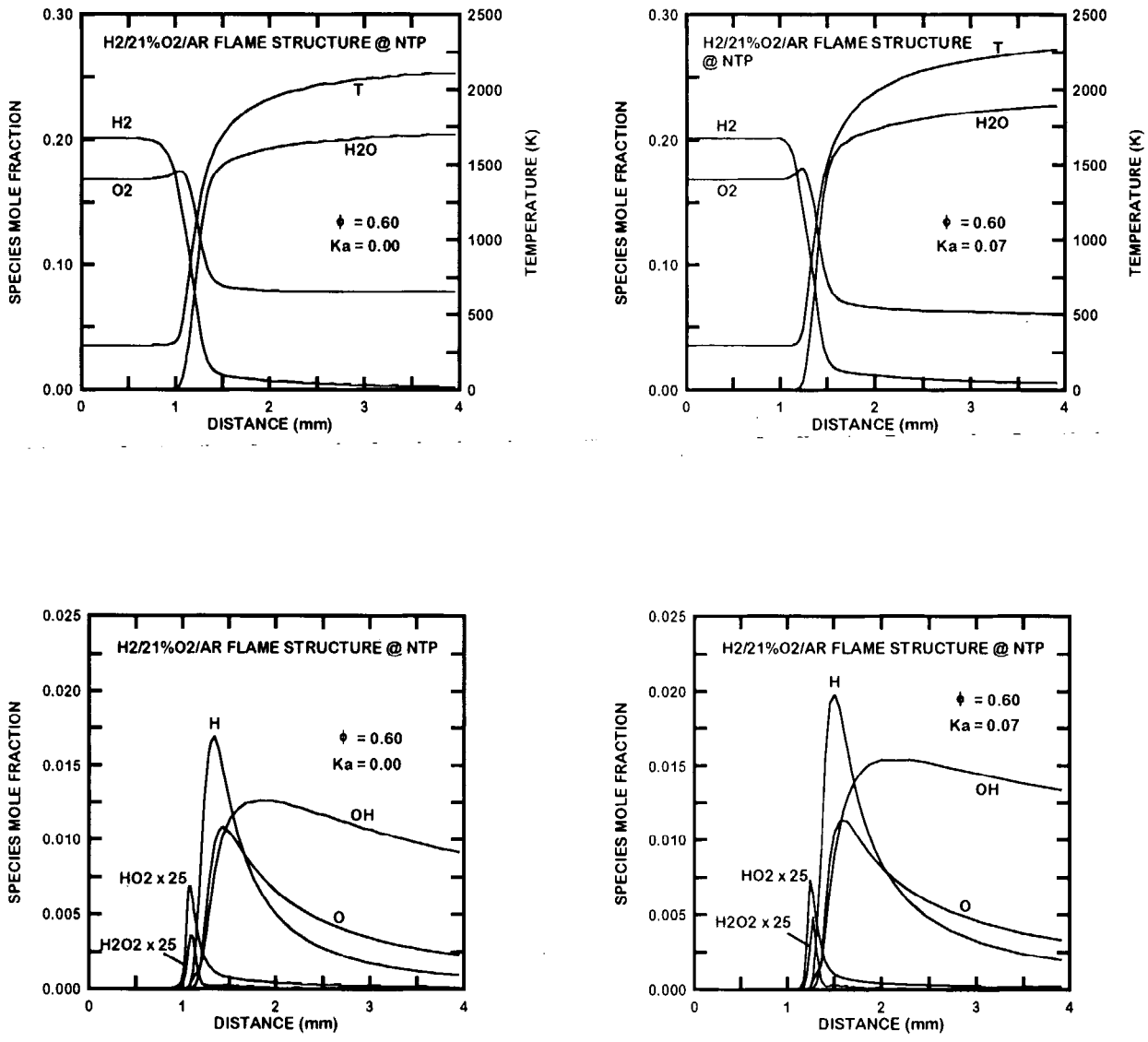

Fig. 7. Predicted flame structure for an unstable condition (H_2/21% O_2/Ar at a fuel-equivalence ratio of 0.6 and NTP).

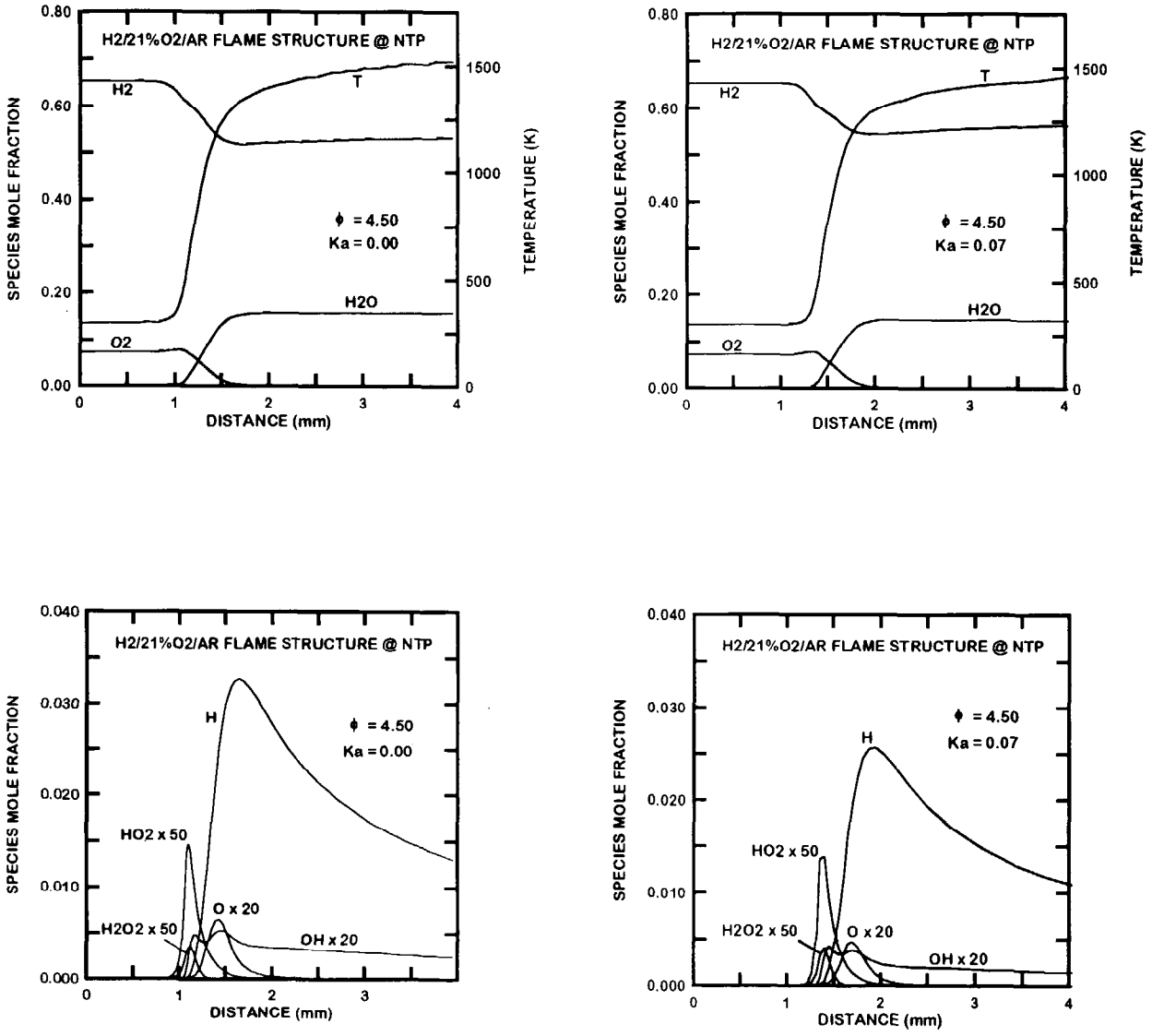

Fig. 8. Predicted flame structure for a stable condition (H_2/21% O_2/Ar flame at a fuel-equivalence ratio of 4.5 and NTP).

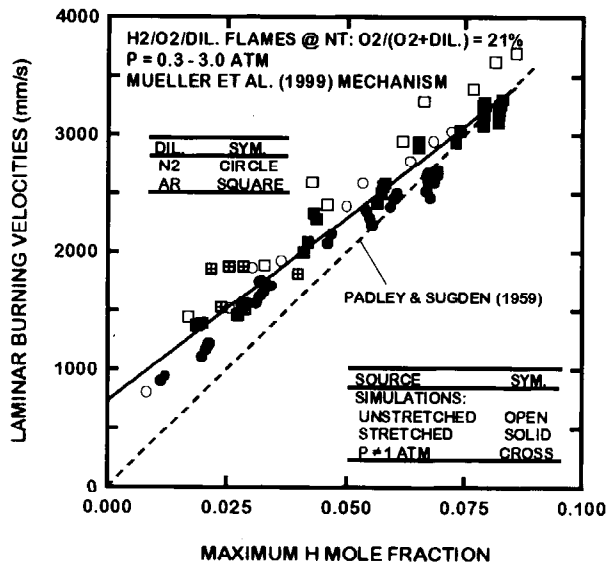

Fig. 9. Laminar burning velocities as a function of maximum H-atom mole fraction for H_2/O_2/diluent flames. Measurements of Padley and Sugden;[35] predictions of the present investigation.

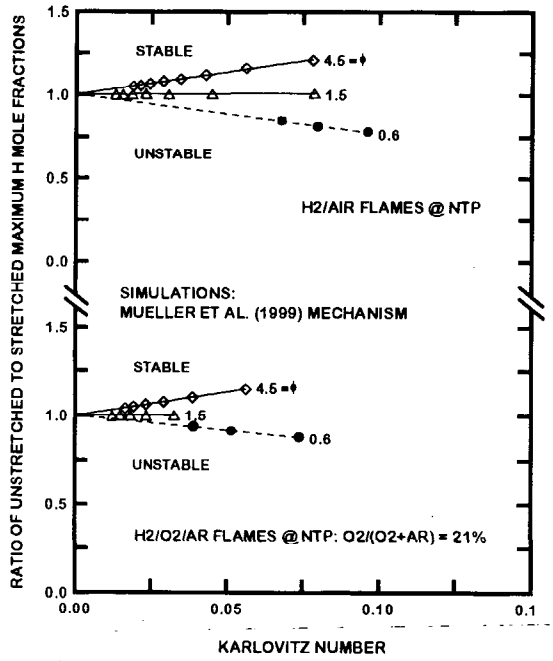

Fig. 10. Predictions of maximum H-atom mole fraction as a function of Karlovitz number and fuel-equivalence ratio for H_2/O_2/diluent flames at NTP.

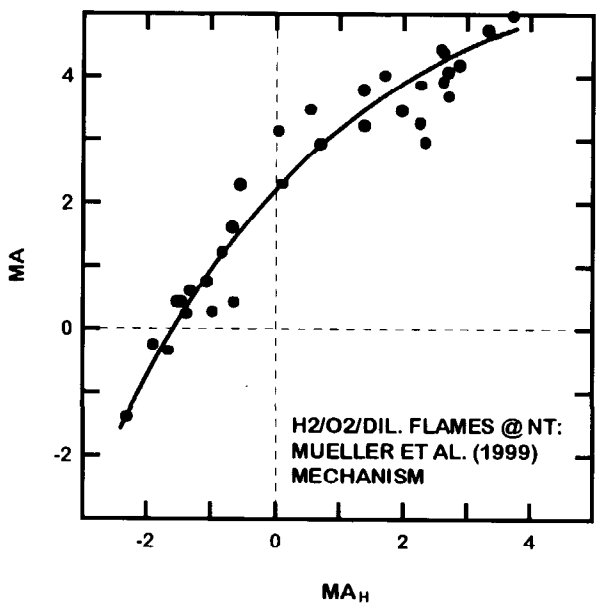

Fig. 11. Correlation between Ma and Ma_H for H_2/O_2/diluent flames at a temperature of 298 K.